Perspective

🔴 Check for updates

Intelligent block copolymer self-assembly towards IoT hardware components

Intelligent block copolymer self-assembly towards IoT hardware components

Geon Gug Yang, Hee Jae Choi, Sheng Li, Jang Hwan Kim, Kyeongha Kwon, Hyeong Min Jin, Bong Hoon Kim[†] and Sang Ouk Kim[†]

[†]e-mail: bonghoonkim@dgist.ac.kr, sangouk.kim@kaist.ac.kr

Supplementary Note 1: BCP self-assembly

Block copolymers (BCPs) are a type of macromolecule composed of chemically distinct polymer chains that are covalently end-linked. The chemical incompatibility of the different polymer blocks leads to phase separation. However, owing to the covalent bonds between the chain ends, the separation is limited to within the length scale of the polymeric molecules, leading to the formation of nanosized domain structures[1–3]. As BCP thin films show highly ordered nanostructures with tunable nanodomain periodicity, they have attracted interest as templates for nanoelectronics fabrication.

The most studied BCPs are linear AB diblock copolymers. The theoretically derived phase diagram (see the figure, panel a) illustrates that the phase behaviour is governed by the volume fraction of the A block (f_A) and the segregation strength parameter (χN, where χ is the Flory–Huggins interaction parameter for the AB monomer pair and N is the total degree of polymerization). Various equilibrium microdomain morphologies have been identified, including lamellae (L), bicontinuous gyroid (G), hexagonally packed cylinders (C), body-centred cubic spheres (S) and close-packed spheres (S_{cp})[4,5].

A key parameter of BCP self-assembly is the length scale or spacing (d) of its periodic nanodomain morphology, which is directly related to the characteristic feature size of the resulting nanopattern. BCP d spacing is generally determined by the polymer molecular chain

size and χ value, following the scaling relationship $d \approx \chi^{1/6} N^{\delta}$, where $\delta = 1/2$ in the weak

segregation limit ($\chi N \approx 10.5$) and $\delta = 2/3$ in the strong segregation limit ($\chi N \gg 10.5$)[5]. For

conventional BCPs with modest χ values (weak segregation) and molecular weights, the

ordered structures typically exhibit d spacings of 10–50 nm[6]. To access nanopatterns with a

broader range of feature sizes, BCPs with different chemistry and chain architectures have been

explored (see the figure, panel b). High-χ BCPs have been exploited for sub-10-nm-scale

ultrafine semiconductor patterning[6]. To fulfill the critical counterbalancing condition for

microphase separation ($\chi N > 10.5$), BCPs with a low N (and thus small feature size structure

of <10 nm) should possess a high χ value for the thermodynamic stabilization of the nanoscale

structures[7,8]. At the other end of the feature size range (> 100 nm), bottlebrush BCPs, composed

of linear backbone and high-density side chain, with high molecular weights are being

investigated[9] for the self-assembly of ordered nanodomains with d spacings exceeding 100 nm.

The ordering kinetics (that defines the speed of the BCP self-assembly and it is thus an essential

processing parameter for high throughput nanopatterning) of bottlebrush BCPs can be much

faster than those of linear BCPs of similar molecular weights, because of their extended chain

conformation and reduced chain entanglements[10].

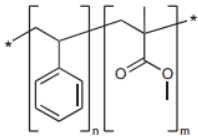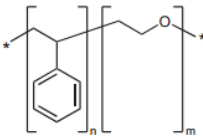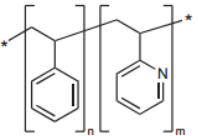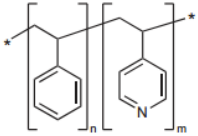**Supplementary Note 2: Directed self-assembly**
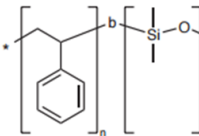
Although BCP thin films self-assemble into nanodomain structures under random thermal

fluctuation, without an external driving force, the lateral ordering of the nanoscale domains is

generally poor and characterized by dense structural defects, such as dislocations and

disclinations[11]. Direct assembly (DSA) strategies have been implemented to create BCP

nanopatterns with a high level of lateral ordering and minimal structural defects. The two most

successful DSA approaches are epitaxial self-assembly[12] and graphoepitaxy[13] (see the figure,

panel c). Epitaxial self-assembly uses chemically pre-patterned surfaces to direct the self-

assembly of BCP thin films and control the lateral ordering of the nanodomains[12,14]. By contrast, graphoepitaxy uses substrates with patterned topographical features[13,15]. Selective wetting of one BCP component to the trench side walls drives the lateral ordering of BCP nanodomains, leading to a well-aligned morphology along the trenches. Although BCP nanopatterns with highly ordered lateral ordering and minimal defects can be achieved by both DSA strategies, the ultimate level of defect control, including dislocation, bridging, and clustering, is a longstanding challenge, especially for the fabrication of delicate and complex semiconductor devices (such as CPU and memory devices).
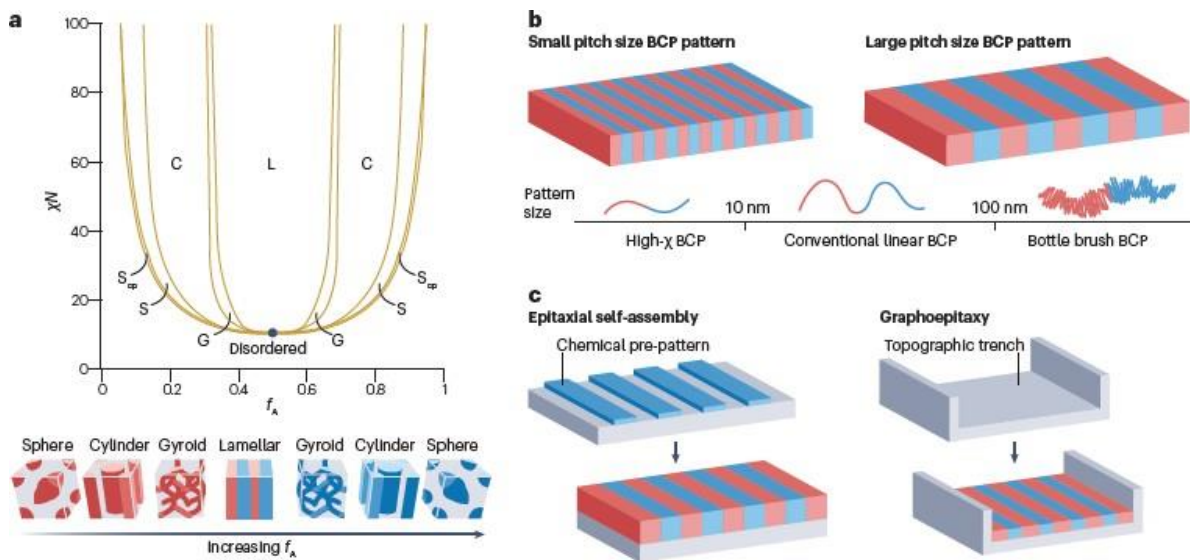
Supplementary Fig. 1| Theoretical thermodynamic phase diagram of diblock copolymer self-assembly**,** tunable self-assembled nanopattern size governed by Flory-Huggins interaction parameter and molecular architecture, DSA strategies by means of epitaxial self-assembly and graphoepitaxy, and widely used BCPs and their characteristics. Panel **a** adapted with permission from ref. 4, American Chemical Society.

Table S1 | Representative types of block copolymer and their chemical structure, characteristics, and IoT device applications. PS-*b*-PMMA has relatively low χ value, so it is easy to induce vertically aligned pattern without topcoat. Moreover, etching rate of PMMA is much faster than PS, enabling facile creation of PS mask pattern for pattern transfer process. In the case of PS-*b*-PEO, hydrophilic PEO block can be swelled by polar solvent and adsorb the ion precursor. Moreover, it forms micelle in the solution, enabling easy fabrication of mesoporous thick film. In the case of PS-*b*-P2VP and PS-*b*-P4VP, pyridinic nitrogen of P2VP and P4VP block can be easily functionalized by proton, resulting in easy metal precursor adsorption and crosslinking. PS-*b*-PDMS has high χ value and inorganic component at PDMS, so it is easy to generate small pitch size pattern with high etching selectivity.

Polymer	PS-*b*-PMMA	PS-*b*-PEO	PS-*b*-P2VP & PS-*b*-P4VP		PS-*b*-PDMS
Chemical Structure					
Character istics	Easy processability Vertical alignment without top-coat Moderate etching selectivity	Versatile precursors decoration Easy to fabricate mesoporous thick films Solution self-assembly using micellization	Metal precursor adsorbability Easy charge modification Solution self-assembly using micellization		High etching selectivity Small pitch size

IoT device	**Sensors** Gas sensor[16–18], biosensor[19–22], IR Sensor[23] **Energy harvesting** Triboelectric nanogenerator[24], thermoelectric nanogenerator[25] Metalens and antireflection coating[26,27] Security systems[28]	**Sensors** Gas sensor[29], biosensor[30] Interactive tactile interfaces[31]	**Sensors** Biosensor[32] **Energy harvesting** Thermoelectric nanogenerator[33,34], osmotic energy conversion[35,36] **User interface** Environment-interactive displays[37–41], anti-reflection coating[42] Security systems[43]	**Sensors** Gas sensor[44] **Energy harvesting** Triboelectric nanogenerator[45]

Supplementary references

1   Park, M., Harrison, C., Chaikin, P. M., Register, R. A. & Adamson, D. H. Block copolymer lithography: periodic arrays of similar to 10(11) holes in 1 square centimeter. *Science* **276**, 1401-1404 (1997).

2   Bates, F. S. & Fredrickson, G. H. Block copolymer thermodynamics - theory and experiment. *Annu. Rev. Phys. Chem.* **41**, 525-557 (1990).

3   Bates, F. S. Polymer-polymer phase-behavior. *Science* **251**, 898-905 (1991).

4   Cochran, E. W., Garcia-Cervera, C. J. & Fredrickson, G. H. Stability of the gyroid phase in diblock copolymers at strong segregation. *Macromolecules* **39**, 2449-2451 (2006).

5   Matsen, M. W. & Bates, F. S. Unifying weak- and strong-segregation block copolymer theories. *Macromolecules* **29**, 1091-1098 (1996).

6   Sinturel, C., Bates, F. S. & Hillmyer, M. A. High χ–low N block polymers: how far can we go?. *ACS Macro Lett.* **4**, 1044–1050 (2015).

7   Jung, Y. S., Chang, J. B., Verploegen, E., Berggren, K. K. & Ross, C. A. A path to ultranarrow patterns using self-assembled lithography. *Nano Lett.* **10**, 1000-1005 (2010).

8   Li, M. Q. & Ober, C. K. Block copolymer patterns and templates. *Mater. Today* **9**, 30-39 (2006).

9   Liberman-Martin, A. L. *et al.* Application of Bottlebrush Block Copolymers as Photonic Crystals. *Macromol. Rapid Commun.* **38**, 1700058 (2017).

10   Xia, Y., Olsen, B. D., Kornfield, J. A. & Grubbs, R. H. Efficient synthesis of narrowly dispersed brush copolymers and study of their assemblies: the importance of side-chain arrangement. *J. Am. Chem. Soc.* **131**, 18525-18532 (2009)

11   Li, W. & Müller, M. Defects in the Self-Assembly of Block Copolymers and Their Relevance for Directed Self-Assembly. *Annu. Rev. Chem. Biomol. Eng.* **6**, 187–216

(2015).

12 Kim, S. O. *et al.* Epitaxial self-assembly of block copolymers on lithographically defined nanopatterned substrates. *Nature* **424**, 411-414 (2003).

13 Bita, I. *et al.* Graphoepitaxy of self-assembled block copolymers on two-dimensional periodic patterned templates. *Science* **321**, 939-943 (2008).

14 Stoykovich, M. P. *et al.* Directed assembly of block copolymer blends into nonregular device-oriented structures. *Science* **308**, 1442-1446 (2005).

15 Segalman, R. A., Yokoyama, H. & Kramer, E. J. Graphoepitaxy of spherical domain block copolymer films. *Adv. Mater.* **13**, 1152-1155 (2001).

16 Yang, G. G. *et al.* Multilevel Self-assembly of block copolymers and polymer colloids for a transparent and sensitive gas sensor platform. *ACS Nano* **16**, 18767-18776 (2022).

17 Yun, T. *et al.* 2D metal chalcogenide nanopatterns by block copolymer lithography. *Adv. Funct. Mater.* **28**, 1804508 (2018).

18 Cagliani, A. et al. Large-area nanopatterned graphene for ultrasensitive gas sensing. *Nano Res.* **7**, 743–754 (2014).

19 Jeong, C. K. *et al.* Electrical biomolecule detection using nanopatterned silicon via block copolymer lithography. *Small* **10**, 337-343 (2014).

20 Park, H. *et al.* Ultrasensitive and selective field-effect transistor-based biosensor created by rings of MoS_2 nanopores. *ACS Nano* **16**, 1826-1835 (2022).

21 Shin, D. O. *et al.* A plasmonic biosensor array by block copolymer lithography. *J. Mater. Chem.* **20**, 7241-7247 (2010).

22 Jin, H. M. *et al.* Ultralarge area sub-10 nm plasmonic nanogap array by block copolymer self-assembly for reliable high-sensitivity SERS. *ACS Appl. Mater.*

Interfaces **10**, 44660-44667 (2018).

23   Park, H. *et al.* A wafer-scale nanoporous 2D active pixel image sensor matrix with high uniformity, high sensitivity, and rapid switching. *Adv. Mater.* **35**, 2210715 (2023).

24   Kim, D. *et al.* High-performance nanopattern triboelectric generator by block copolymer lithography. *Nano Energy* **12**, 331-338 (2015).

25   Zhou, C. *et al.* Enhanced reduction of thermal conductivity in amorphous silicon nitride-containing phononic crystals fabricated using directed self-assembly of block copolymers. *ACS Nano* **14**, 6980-6989 (2020).

26   Kim, J. Y. *et al.* Highly tunable refractive index visible-light metasurface from block copolymer self-assembly. *Nat. Commun.* **7**, 12911 (2016).

27   Rahman, A. *et al.* Sub-50-nm self-assembled nanotextures for enhanced broadband antireflection in silicon solar cells. *Nat. Commun.* **6**, 5963 (2015).

28   Kim, J. H. *et al.* Nanoscale physical unclonable function labels based on block copolymer self-assembly. *Nat. Electron.* **5**, 433-442 (2022).

29   Wang, J. L. & Yu, S. H. Janus Mesostructures for Simultaneous Multivariable Gases Sensors. *Matter* **1**, 1110–1111 (2019).

30   Akinoglu, G. E., Mir, S. H., Gatensby, R., Rydzek, G. & Mokarian-Tabari, P. Block Copolymer Derived Vertically Coupled Plasmonic Arrays for Surface-Enhanced Raman Spectroscopy. *ACS Appl. Mater. Interfaces* **12**, 23410–23416 (2020).

31   Lang, C. *et al.* Nanostructured block copolymer muscles. *Nat. Nanotechnol.* **17**, 752-758 (2022).

32   Cha, S. K. *et al.* Au–Ag core–shell nanoparticle array by block copolymer lithography

for synergistic broadband plasmonic properties. *ACS Nano* **9**, 5536-5543 (2015).

33   Oh, J. *et al.* Significantly reduced thermal conductivity and enhanced thermoelectric properties of single- and bi-layer graphene nanomeshes with sub-10 nm neck-width. *Nano Energy* **35**, 26-35 (2017).

34   Tang, J. Y. *et al.* Holey silicon as an efficient thermoelectric material. *Nano Lett.* **10**, 4279-4283 (2010).

35   Lin, X. *et al.* Heterogeneous MXene/PS-b-P2VP nanofluidic membranes with controllable ion transport for osmotic energy conversion. *Adv. Funct. Mater.* **31**, 2105013 (2021).

36   Zhang, Z. *et al.* Ultrathin and ion-selective janus membranes for high-performance osmotic energy conversion. *J. Am. Chem. Soc.* **139**, 8905-8914 (2017).

37   Kang, Y., Walish, J. J., Gorishnyy, T. & Thomas, E. L. Broad-wavelength-range chemically tunable block-copolymer photonic gels. *Nat. Mater.* **6**, 957-960 (2007).

38   Kang, H. S. *et al.* 3D touchless multiorder reflection structural color sensing display. *Sci. Adv.* **6**, eabb5769 (2020).

39   Kim, T. et al. Self-powered finger motion-sensing structural color display enabled by block copolymer photonic crystal. *Nano Energy* **92,** 106688 (2022).

40   Zhang, R., Qiang, Z., Wang, M. Integration of Polymer Synthesis and Self-Assembly for Controlled Periodicity and Photonic Properties. *Adv. Funct. Mater.* **31,** 2005819 (2021).

41   Park, T. H. et al. Block copolymer structural color strain sensor. *NPG Asia Mater.* **10,** 328–339 (2018).

42   Mokarian-Tabari, P. *et al.* Large block copolymer self-Assembly for fabrication of subwavelength nanostructures for applications in optics. *Nano Lett.* **17**, 2973-2978 (2017).

43   Tang, Z. L. *et al.* Unclonable anti-counterfeiting labels based on plasmonic-patterned manostructures. *Adv. Eng. Mater.* **24**, 2101701 (2022).

44   Jung, Y. S., Jung, W., Tuller, H. L. & Ross, C. A. Nanowire conductive polymer gas sensor patterned using self-assembled block copolymer lithography. *Nano Lett.* **8**, 3776-3780 (2008).

45   Jeong, C. K. *et al.* Topographically-designed triboelectric nanogenerator via block copolymer self-assembly. *Nano Lett.* **14**, 7031-7038 (2014).